

# ***B*-hadron cross-section measurement in *pp* collisions at $\sqrt{s} = 14$ TeV with the ALICE muon spectrometer**

**L. Manceau<sup>a</sup>**  
for the ALICE Collaboration

Laboratoire de Physique Corpusculaire (CNRS/IN2P3), Université Blaise Pascal, 24, Av. des Landais, 63177 Aubière, France

Received: 29 September 2008 / Revised: 28 January 2009 / Published online: 17 February 2009  
© Springer-Verlag / Società Italiana di Fisica 2009

**Abstract** ALICE (A Large Ion Collider Experiment) is the LHC detector designed to measure nucleus-nucleus (AA) collisions where the formation of the Quark Gluon Plasma is expected. The experiment will also study proton-proton (*pp*) collisions at 14 TeV. Amongst the relevant observables to be investigated in *pp* collisions, the *B*-hadron cross-section is particularly interesting since it provides benchmarks for theoretical models and it is mandatory for understanding heavy flavour production in AA collisions. The performances of the ALICE muon spectrometer to measure *B*-hadron cross-section in *pp* collisions at 14 TeV via single muons are presented.

**PACS** 25.75.-q · 12.38.Mh · 25.75.Nq

## **1 Introduction**

The prime goal of relativistic heavy-ion collisions is to study QCD matter in extreme conditions of temperature. With a nucleon-nucleon center-of-mass energy of  $\sqrt{s_{NN}} = 5.5$  TeV which exceeds the one reached at RHIC by about a factor 30, the LHC (Large Hadron Collider) will bring new insights in heavy-ion physics. The energy density should reach 15–60 GeV/fm<sup>3</sup>. At such energy densities, QGP is expected to be created.

One of the most important aspects of this energy range will be the abundant production of hard probes which could be used, for the first time, as high statistics probes of the medium. The charm and beauty production cross-section (see Table 1.1) should be 10 and 100 times, respectively, larger than at RHIC [1].

The main motivation to measure the *B*-hadron cross-section in *pp* collisions is to test Next-to-Leading-Order

**Table 1.1** NLO pQCD predictions in *pp* collisions at  $\sqrt{s} = 14$  TeV for the number of charm and beauty quark-antiquark pairs per event and corresponding production cross-section [2]

	$N/\text{evt.}$	$\sigma_{Q\bar{Q}}$ (mb)
$c\bar{c}$	0.16	11.2
$b\bar{b}$	0.0072	0.51

perturbative QCD (NLO pQCD) calculations which still predict cross-sections with large uncertainties [3]. Measuring the *B*-hadron cross section in *pp* collisions is also mandatory for understanding:

- *B*-hadron cross-section in *pA* collisions, where the study of shadowing and anti-shadowing should give information on gluon Parton Distribution Functions (PDF) in the nucleus;
- *B*-hadron cross-section in AA collisions where the study of heavy flavour energy loss through hot QCD matter should give information on the initial density of gluons and on the dissipative properties of the medium. One can mention that one expects that light quarks exhibit a weak sensitivity to these effects. Indeed, they lose more energy than heavy quarks;
- production cross-sections of bottomonia in *pp*, *pA* and AA collisions;
- production cross-section of secondary  $J/\psi$  in *pp* collisions which is a benchmark for understanding its production in *pA* and AA collisions.<sup>1</sup>

## **2 The ALICE detector**

ALICE (A Large Ion Collider Experiment) is the LHC experiment dedicated to the study of nucleus-nucleus col-

<sup>a</sup> e-mail: loic.manceau@clermont.in2p3.fr

<sup>1</sup> The ratio of secondary  $J/\psi$  from *B*-hadron decay to direct  $J/\psi$  is expected to reach 20% at the LHC (assuming no hot medium effects).

lisions [4]. More than 1000 collaborators from about 30 countries are presently participating to ALICE. The ALICE experiment is designed to perform simultaneous and high precision measurements of numerous observables based on hadrons, leptons and photons, in a broad acceptance.

The detector consists of a central barrel, a forward muon spectrometer and forward/backward small acceptance detectors. The central barrel of ALICE is made of four layers of detectors placed in the solenoidal field ( $B < 0.5$  T) provided by the L3 magnet. From the inner side to the outer side, these detectors are (i) the Inner Tracker System (ITS) consisting of six layers of silicon detectors, (ii) the large-volume Time Projection Chamber (TPC), (iii) the high-granularity Transition Radiation Detector (TRD) and (iv) the high-resolution Time of Flight system (TOF) based on multi-gap resistive plate chambers. They provide charged particle reconstruction and identification in the pseudo-rapidity range  $|\eta| < 0.9$ , with full azimuthal coverage and a broad transverse momentum ( $p_t$ ) acceptance. The ALICE central barrel will later also be equipped with a large acceptance ( $|\eta| < 1.4$ ,  $\Delta\Phi = 110^\circ$ ) Electro-Magnetic CALorimeter (EMCAL). These large area devices are complemented by two smaller acceptance detectors: the High Momentum Particle IDentification (HMPID) and the PHOTon Spectrometer (PHOS). In the forward/backward region, additional detectors allow fast characterization and selection of the events as well as charged particle measurement in the pseudo-rapidity ranges  $-3.4 < \eta < -1.7$  and  $1.7 < \eta < 5.0$ . The Photon Multiplicity Detector (PMD) will measure photon multiplicity in the pseudo-rapidity range  $1.8 < \eta < 2.6$ . At large rapidities, spectator nucleons in heavy-ion collisions will be measured by the Zero-Degree Calorimeters. Finally a forward muon spectrometer [5] covering the pseudo-rapidity range  $-4 < \eta < -2.5$  complements the central part. It consists of a front absorber, a dipole magnet, ten high-granularity tracking chambers, a muon filter and four large area trigger chambers.

### 3 Simulation inputs

We use the simulated data produced within the Physics Data Challenge 2006 (PDC06) via the computing grid. Events have been simulated and reconstructed with the AliRoot framework [6]. The simulation is done by means of the PYTHIA 6.2 Monte Carlo event generator with CTEQ5L PDFs (parameters are described in [1]). In order to optimize the statistics and to reduce the computing time, events were reconstructed only if at least one muon with  $p_t$  larger than  $0.5$  GeV/c is produced in the acceptance of the muon spectrometer. This cut is applied at the generation of the events, when  $\pi$  and  $K$  are not yet desintegrated in muons. Thus, the yield of muons from light hadron decays is strongly underestimated. In the analysis presented here, we focus on

$p_t > 2$  GeV/c range and background from  $\pi$ ,  $K$  decay is perfectly subtracted. The reconstructed muon distributions then consist exclusively of muons from charm and beauty decay. These are corrected for detection efficiency by means of the method described in [7, 8]. The mean value of the efficiency is about 96%.

Whereas the Pythia setting in the PDC06 simulations allows to consistently reproduce the beauty production cross-section as predicted by NLO pQCD calculations (Table 1.1), it underestimates the charm production cross-section by a factor  $\sim 2$ . This is taken into account by scaling up the muon distributions accordingly. Furthermore, the statistics available in the PDC06 production allows to exploit the muon  $p_t$  distribution up to  $\sim 10$  GeV/c only. In order to compensate for this lack of statistics, the muon distributions have been fitted and then extrapolated up to  $p_t = 20$  GeV/c. A successful description of the muon  $p_t$  distributions is obtained for both charm and beauty with the following function [1]:

$$f = a \times \frac{1}{(1 + (\frac{p_t}{b})^2)^c} \quad (3.1)$$

where  $a$ ,  $b$  and  $c$  are free parameters. Note that beyond  $p_t = 20$  GeV/c muons from  $W^\pm$  decay dominate [9]. Figure 3.1 shows the  $p_t$  distributions of muons from  $D$  and  $B$ -hadron decays scaled and extrapolated as described previously. The charm/beauty crossing point is located at  $p_t \sim 6$  GeV/c. Beauty dominates at high transverse momentum and charm dominates at low transverse momentum. It is worth noticing that the value of the crossing point depends on the quark masses, the QCD factorization and renormalization scales, the fragmentation functions and the PDFs. For example, using the inputs provided in the report by the joined HERA-LHC groups [3], a shift of the crossing point by approximately  $\pm 2$  GeV/c is expected.

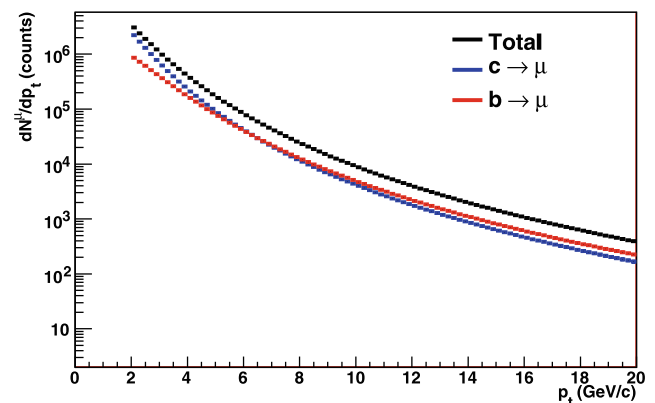


**Fig. 3.1** Transverse momentum distributions of muons from  $c$  and  $b$  quark decays (statistics from scenario 1, see Sect. 5)

#### 4 Method

The method to extract the differential inclusive  $B$ -hadron cross-section is widely used and well documented. It was developed by the UA1 Collaboration [10, 11] and is used by the CDF [12] and the D0 [13] Collaborations. It has also been used by the ALICE Collaboration to investigate the feasibility of measuring the  $B$ -hadron cross-section in  $pp$  collisions at  $\sqrt{s} = 14$  TeV with single electrons [14], in Pb–Pb collisions at  $\sqrt{s_{NN}} = 5.5$  TeV with single electrons [15], single muons and dimuons [16]. This method consists in three steps:

1. Extraction of the number of muons from  $b$  semileptonic decays by performing a combined fit of the muon  $p_t$  distribution. The fitting function is:

$$(T - B)(f_c + R \times f_b). \quad (4.1)$$

In this formula,  $T$  is the total number of muons,  $B$  is the number of muons from  $b$  semileptonic decays (it is a free parameter),  $f_c$  and  $f_b$  are model dependent shapes of the  $p_t$  distribution of muons from  $c$  and  $b$  semileptonic decays, respectively;  $R$  is the number of muons from  $b$  semileptonic decays over the number of muons from  $c$  semileptonic decays (it is a free parameter fixed within 30% as we assume that models [3] predict  $R$  with uncertainties smaller than 30%).

2. Correction of this number of muons for integrated luminosity ( $\int L dt$ ), detection efficiency ( $\epsilon$ ), acceptance and decay kinematics ( $F(\mu \leftarrow B)$ ). This correction is achieved according to (4.2). The  $F(\mu \leftarrow B)$  factor is obtained from a Monte Carlo simulation.

$$\begin{aligned} \sigma^B &= \frac{d\sigma^B}{d\eta}(p_t^B > p_t^{min})|_{-4 \leq \eta \leq -2.5} \\ &= \frac{N_{\mu \leftarrow B}(\Phi^\mu)}{\int L dt} \times \frac{1}{\epsilon} \\ &\quad \times \left[ \frac{\frac{d\sigma^B}{d\eta}(p_t^B > p_t^{min})|_{-4 \leq \eta \leq -2.5}}{\sigma^B(\Phi^\mu)} \right]_{MC} \\ &= \frac{N_{\mu \leftarrow B}(\Phi^\mu)}{\int L dt} \times \frac{1}{\epsilon} \times F(\mu \leftarrow B). \end{aligned} \quad (4.2)$$

In (4.2) (i)  $\frac{d\sigma^B}{d\eta}(p_t^B > p_t^{min})|_{-4 \leq \eta \leq -2.5}$  is the integral of the  $p_t$  spectrum of  $B$ -hadrons with rapidity  $-4 \leq \eta \leq -2.5$  and  $p_t^B > p_t^{min}$ , (ii)  $\sigma^B(\Phi^\mu)$  is the integral of the  $p_t$  distribution of  $B$ -hadrons decaying into muons within a given phase space  $\Phi^\mu$  ( $-4 \leq \eta \leq -2.5$ ,  $p_t^\mu \geq 4$  GeV/c and a given  $p_t^\mu$  range), and (iii)  $p_t^{min}$  is defined such that 90% of accepted  $B$ -hadrons have a  $p_t$  larger than that value (see Fig. 4.1). We choose this definition to minimize the acceptance and decay kinematics correction dependence on shapes used in Pythia for the Monte Carlo computation of  $F(\mu \leftarrow B)$ .

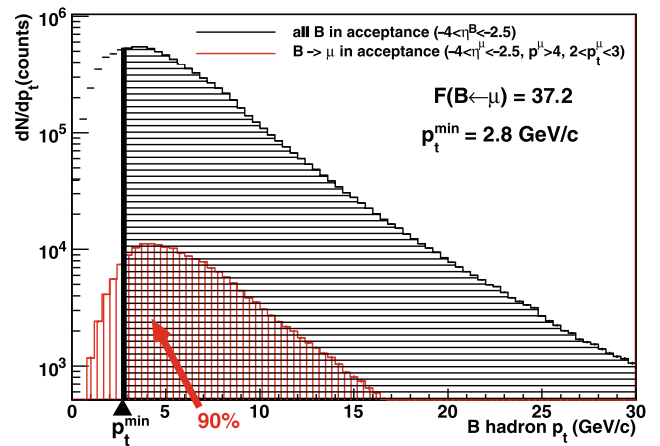


**Fig. 4.1** Illustration of  $F(\mu \leftarrow B)$  computation. Horizontal line area: inclusive  $B$ -hadron production in the acceptance. Vertical line area:  $B$  hadrons which yield muons of  $2 \leq p_t \leq 3$  GeV/c in the acceptance of the spectrometer

3. Repetition of step one and two for different  $\Phi^\mu$  (i.e. different  $p_t^\mu$  ranges) to extract differential inclusive  $B$ -hadron cross-section (Fig. 7.1).

#### 5 Expected yields

We performed statistics estimates for three different scenarios of data taking:

- scenario 1: one month of data taking at low luminosity,  $L = 10^{30} \text{ cm}^{-2} \text{ s}^{-1}$ ,  $t = 10^6 \text{ s}$ ;
- scenario 2: one month of data taking at nominal luminosity,  $L = 3 \times 10^{30} \text{ cm}^{-2} \text{ s}^{-1}$ ,  $t = 10^6 \text{ s}$ ;
- scenario 3 (nominal scenario): one year of data taking at nominal luminosity,  $L = 3 \times 10^{30} \text{ cm}^{-2} \text{ s}^{-1}$ ,  $t = 10^7 \text{ s}$ .

Figure 5.1 shows that the muon yield is large over a broad  $p_t$  range even in scenario 1. This yield leads to low statistical

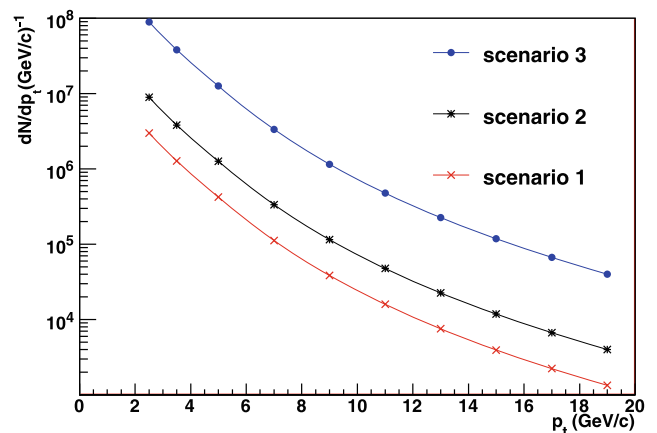


**Fig. 5.1** Muon yield versus  $p_t$  for the three scenarios of data taking described in the text

uncertainties. Even in scenario 1 at a  $p_t$  of 20 GeV/c, the relative statistical uncertainty is as low as 2%. The  $p_t$  range shown in Fig. 5.1 goes from 2 to 20 GeV/c. Indeed, below 2 and beyond 20 GeV/c muons from  $\pi$ ,  $K$  and  $W$  decay dominate, respectively.

## 6 Systematic uncertainties

In order to determine the systematic uncertainties from the method, we have used NLO pQCD predictions with different assumptions on the quark masses, the QCD factorization and renormalization scales and the PDFs [3]. As these predictions are available at the hadron level only, we have first performed Pythia simulations in order to reproduce them. Then, we have extracted from the corresponding decay muon  $p_t$  distributions biased  $f_c$  and  $f_b$  shapes. The latter are used as inputs for the combined fit from which we have extracted the systematic uncertainties. Figure 6.1 shows two examples of fits obtained with

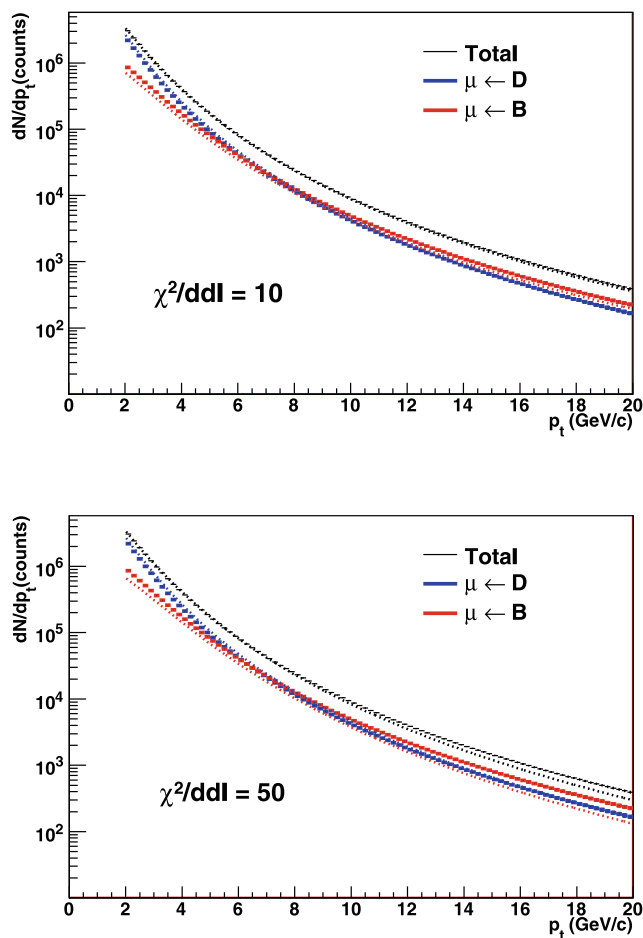


**Fig. 6.1** Examples of combined fits for two combinations of biased shapes as described in the text. The dotted lines show the result of the fit and the histograms are input distributions. The  $\chi^2$  of the fits are reported on the plots

these biased  $f_c$  and  $f_b$  shapes. The systematic uncertainties run from 17% to 22%. It is important to note from Fig. 6.1 that the  $\chi^2$  gives a good indication of the fit quality and should therefore allow to constrain the systematics.

## 7 Inclusive differential $B$ -hadron cross-section

Figure 7.1 shows the inclusive differential  $B$ -hadron cross-section. As it can be seen, the input (histogram) is well reconstructed (squares). Statistical errors are negligible (Sect. 5). The main source of uncertainties is the systematics from the fit (Sect. 6) which is about 20%. As the choice of  $p_t^{\min}$  (Sect. 4) minimize the  $F(\mu \leftarrow B)$  dependence on shapes used in Pythia the systematic errors from  $F(\mu \leftarrow B)$  are negligible. Statistical errors from  $F(\mu \leftarrow B)$  run from 0.4% to 15%. Note that this error can be further reduced since it only depends on the Monte-Carlo simulation used for computing the  $F(\mu \leftarrow B)$  factor. A 5% normalisation uncertainty (uncertainties on luminosity,  $pp$  cross-section) is not included in Fig. 7.1.

## 8 Conclusion

The  $B$ -hadron cross-section in  $pp$  collisions is an essential measurement for a number of physics items in  $pp$ ,  $pA$  as well as in  $AA$  collisions at the LHC. We have shown that this measurement can be successfully performed from single muons in  $pp$  collisions at  $\sqrt{s} = 14$  TeV using a method first developed by the UA1 Collaboration and further used by the CDF and the D0 Collaborations. The inclusive differential  $B$ -hadron cross-section can be reconstructed from low  $p_t$  up to  $p_t \sim 20$  GeV/c. The statistical error is negligible and the systematic one is of the order of 20%. In the

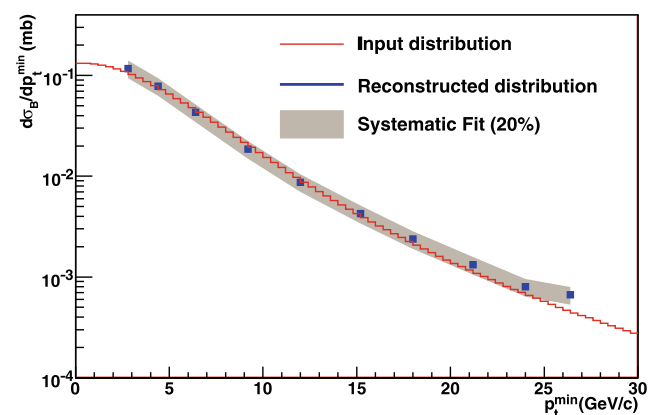


**Fig. 7.1** Inclusive differential  $B$ -hadron cross-section. The histogram (squares) shows the input (reconstructed) distribution. The shaded area shows systematic errors estimated to  $\sim 20\%$

present work the contribution from muons from  $\pi$ ,  $K$  decays were assumed to be negligible. In the next steps, a realistic background subtraction should be performed. We note that the same method can be applied in the electron channel in the central barrel of the ALICE experiment with different statistical and systematical uncertainties. Thus, performing the two analysis will provide useful cross-checks. We finally note that the  $D$ -hadron cross-section can be simultaneously extracted with the exposed method.

## References

1. B. Alessandro et al. (ALICE Collaboration), J. Phys. G **32**, 1295 (2006)
2. M.L. Mangano, P. Nason, G. Ridolfi, Nucl. Phys. B **373**, 295 (1992)
3. J. Baines et al., [arXiv:hep-ph/0601164](https://arxiv.org/abs/hep-ph/0601164)
4. F. Carminati et al. (ALICE Collaboration), J. Phys. G **30**, 1517 (2004)
5. C. Finck et al. (ALICE Muon Spectrometer Collaboration), J. Phys.: Conf. Ser **50**, 397–401 (2006)
6. Alice Experiment: Offline Project. <http://aliceinfo.cern.ch/Offline>
7. Z. Conesa del Valle, L. Aphecetche, G. Martinez Garcia, Ch. Finck, Efficiency determination strategy in the ALICE muon spectrometer. ALICE Collaboration internal note to be published
8. Z. Conesa del Valle, Performance of the ALICE muon spectrometer. Weak boson production and measurement in heavy-ion collisions at LHC. PhD Dissertation
9. Z. Conesa del Valle, A. Dainese, H.T. Ding, G. Martinez Garcia, D.C. Zhou, Phys. Lett. B **663**, 202 (2008). [arXiv:0712.0051](https://arxiv.org/abs/0712.0051) [hep-ph]
10. C. Albajar et al. (UA1 Collaboration), Phys. Lett. B **213**, 405 (1988)
11. C. Albajar et al. (UA1 Collaboration), Phys. Lett. B **256**, 121 (1991) [Erratum: Phys. Lett. B **262**, 497 (1991)]
12. F. Abe et al. (CDF Collaboration), Phys. Rev. Lett. **71**, 500 (1993)
13. B. Abbott et al. (D0 Collaboration), Phys. Lett. B **487**, 264 (2000) [arXiv:hep-ex/9905024](https://arxiv.org/abs/hep-ex/9905024)
14. F. Antinori et al. ALICE Collaboration internal note ALICE-INT-2006-015
15. F. Antinori et al., ALICE Collaboration internal note ALICE-INT-2005-33
16. R. Guernane et al., ALICE Collaboration internal note ALICE-INT-2005-018